

solder protects underlying tissue from damage due to excess laser-induced heat deposited in the tissue. Our protein solder consists of a high concentration solution of bovine serum albumin, mixed with indocyanine green dye to enhance the solder's absorption of the 800-nm diode laser light used to activate the solder.¹ The solder is formed into hollow tubes and pre-heat treated to enhance its stability and strength during and immediately after surgery. The fold-and-bond surgical technique we have used to repair blood vessels with the protein solder is based on a technique reported early this century.²

A total of 90 rats were divided into two groups. In group one, the repairs were performed using conventional microsuturing techniques, and in group two, the repairs were performed using our new laser welding technique. In addition, subgroups of animals from each group were evaluated at times of 10 min, 1 hour, 1 day, 1 week and 6 weeks, after surgery. The time the aorta was clamped was noted for each procedure and the results analysed statistically. Subsequently, after the selected evaluation period, each repair was tested for patency and mechanical strength. Furthermore, three animals from each subgroup were sacrificed to allow histological examination of the surgical repair site.

All repairs were patent at the time of evaluation. The mean clamp time of all repairs performed by microsuturing was 20.6 minutes, compared to the mean clamp time of all laser soldered repairs of 7.2 minutes ($p < 0.0001$). The strain measurements revealed a stronger mechanical bond of the sutured repair in the initial phase, but after six weeks, the mechanical resistance was comparable for both techniques. Histological evaluations indicated that the solder was resorbed by the body after 6 weeks, and that negligible thermal damage occurred to surrounding tissue.

In conclusion, our new technique using a resorbable protein as a solder activated by a diode laser provides a reliable safe rapid arterial repair, which could be performed faster than conventional suturing after a short learning curve.

We acknowledge funding by the Australian Research Council, Macquarie University and the Microsearch Foundation of Australia.

*Former address: Univ. of Vienna Medical School, Austria.

**Macquarie Univ., Australia

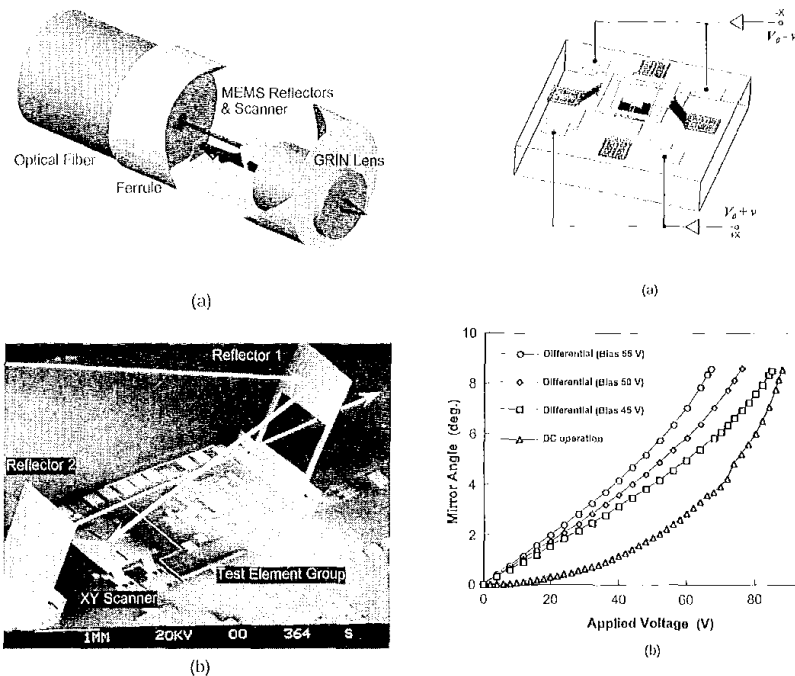
1. A. Iauto, R. Trickett, R. Malik, J. Dawes, E. Owen, *Las. Surg. Med.* **21**, 134 (1997).
2. E. Payr, *Arch. Klin. Chir.* **62**, 67 (1900).

CThL3 10:45 am

Surface-micromachined confocal scanning optical microscope

W. Piyawattanametha, I.I. Toshiyoshi,* J. LaCrosse,** M.C. Wu, *Electrical Engineering Department, Univ. of California, Los Angeles, 66-147D, Engineering IV, Box 951594, Los Angeles, California 90095-1594, USA; E-mail: wu@icsl.ucla.edu*

The confocal scanning microscope (CSM) can create high-resolution three-dimensional

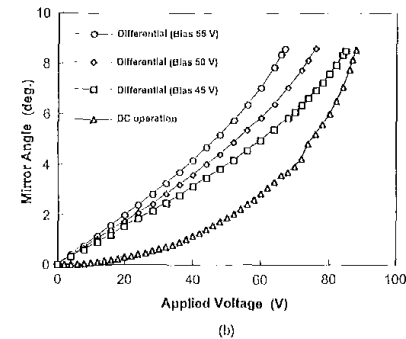


CThL3 Fig. 1. (a) Schematic of μCSOM endoscope and (b) surface micromachined optical scanner and reflectors.

(3D) images of thick and light-scattering objects from successive acquisition of 2D images through its optical sectioning property. This capability allows us to develop a micro-optical-endoscope for high-quality *in vivo* imaging of living tissue. Earlier works on CSMS employed a single-mode optical fiber for illumination and detection. Reported scanning methods utilize either fiber movement or lens translation, which are not fast enough to minimize motion artifacts or suitable for further miniaturization. The microelectromechanical system (MEMS) approach has shown great promise to produce miniaturized CSMS by batch fabrication. For example, Ref. 1 describes two cascaded 1D scanning mirrors made by silicon bulk-micromachining.

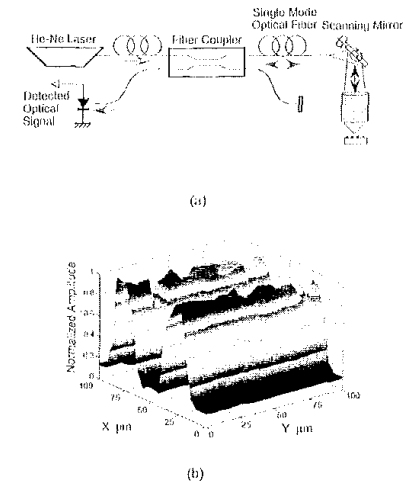
In this paper, we propose a novel surface-micromachined 2D scanner to extend the performance of CSMS. This microscope is called surface-micromachined confocal scanning optical microscope (μCSOM). Surface-micromachining technique takes advantage of the MEMS free-space micro-optical bench (FS-MOB),² which provides more flexibility in integrating micro-optics with other MEMS or optical components.

The schematic of the μCSOM endoscope is illustrated in Fig. 1(a). A MEMS chip with fixed reflectors and a scanning mirror is placed in front of a single-mode fiber. The probing light is projected and collected by a lens. We used a gradient-index (GRIN) lens for its small diameter (1.8 mm), low spherical aberration, high coupling efficiency, and very high numerical aperture (0.46). The 3D structure of the scanning mirror and reflectors were realized by the Micro-Elevator by Self-Assembly (MESA) technique,³ as illustrated in Fig. 1(b). The gold-finished polysilicon scanning mirror



CThL3 Fig. 2. (a) SEM view showing the driving electrodes for electrostatic differential operation and (b) plot of mirror angle as a function of applied voltage. Differential operation at biasing voltages of 45, 50, and 55 V show improved linearity than that of DC operation.

(400 μm × 400 μm) is suspended with nested XY-torsion beams (2-μm wide, 200-μm long, and 1.5-μm thick) 72 μm above four driving electrodes tiled on the substrate. This architecture enables a wide scan range of ±10° for X-scan and ±20° for Y-scan. The angle-voltage transfer curve was linearized by applying a DC bias voltage, V_0 , plus a small signal differential voltage, $\pm v$, as illustrated in Fig. 2. Note that the bias voltage can be used to tune the slope of the curve. The resonant frequency of the 2D scanner is 1 kHz, and the magnitude of wobble



CThL3 Fig. 3. (a) μCSOM experimental setup and (b) 3D plot of intensity distribution from 25-μm pitch line-and-space metallic patterns.

and jitter are 22 μrad and 85 μrad , respectively. The pointing accuracy is less than 3.3 μrad .

We have demonstrated the μCSOM using a monochromatic light source at 633-nm wavelength and a GRIN lens with a 2-mm working distance. A 3D intensity plot of a sample specimen (25- μm pitch line-and-space metallic patterns) is illustrated in Fig. 3. The field of view of the μCSOM was 100 $\mu\text{m} \times 100 \mu\text{m}$. Square-mesh scanning without XY cross talk was performed by using a calibration table programmed on a personal computer. It achieved a transverse resolution of 5- μm FWHM and an axial resolution of 80 μm FWHM. The spot size is larger than the theoretical limit (2.5 μm) due to the mirror's curvature (2-mm radius of curvature).

*Inst. of Industrial Science, The Univ. of Tokyo, Japan

**Spectra-Physics, USA

1. D.L. Dickensheets, G.S. Kino, "Silicon-micromachined scanning confocal optical microscope," *IEEE J. Microelectromech. Syst.* **7**, 38–37 (1998).
2. M.C. Wu, "Micromachining for optical and optoelectronic systems," in *Proc. IEEE* **85**, No. 11, 1833–1856 (November 1997).
3. Li Pan, M.C. Wu, Kent D. Choquette, M.H. Crawford, "Self-assembled microactuated XYZ stages for optical scanning and alignment," *Proc. of International Solid State Sensors and Actuators Conference (Transducers'97)*, Chicago, IL, USA, June 16–19, vol. 1, pp. 319–322 (1997).

CThL4

11:00 am

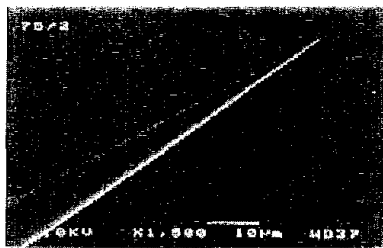
Fiber-optic microsensors to measure backscattered light intensity in biofilms

H. Beyenal, Z. Lewandowski, C. Yakymyshyn,* B. Lemley,* J. Wehri,* *Ctr. for Biofilm Engineering, Montana State Univ., Bozeman, Montana 59717, USA; E-mail: ZL@erc.montana.edu*

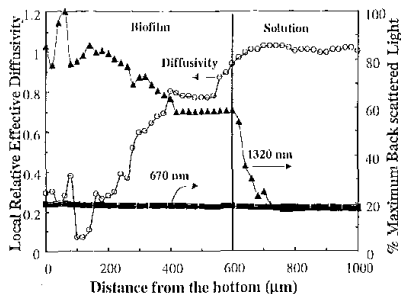
Biofilms are a predominant microbial growth mode in natural and engineered systems.¹ Biofilm processes are implicated in bioremediation of toxic compounds,² oral hygiene,³ souring of oil formations,⁴ microbially influenced corrosion,⁵ and infection of prosthetic devices.⁶ To evaluate metabolic activity of biofilm microorganisms it is imperative to measure chemical gradients of nutrient concentration across microbial deposits less than a few hundred microns thick. Presently, electrochemical microsensors are used with tip diameters not exceeding a few 10's of microns.

Micro-scale fiber-optic sensors⁷ have several potential advantages. They are immune to electromagnetic noise, need no reference electrodes and are easier to fabricate. We have developed a fiber-optic microsensor based on commercially available optical telecommunications components that measures backscattered light from a tapered fiber tip.

The biofilm preparation and standard measurement techniques are described elsewhere.^{8,9} A 670-nm or 1320-nm Fabry-Perot laser diode operated below threshold was



CThL4 Fig. 1. SEM micrograph of fiber-optic microsensor tip.



CThL4 Fig. 2. The variation in the % of maximum back-scattered light intensity (670-nm and 1320-nm wavelengths) and local relative effective diffusivity by depth in a heterogeneous biofilm at the same location.

coupled through a 2 \times 2, 50:50 single-mode fiber coupler. One arm of the coupler was monitored using a PIN diode. The other coupler output was connected to a short section of single-mode fiber with a tapered end. Any backscattered light was collected by a second PIN diode. Data was recorded as the ratio between the backscattered and reference signals.

Tapered tips were formed by wet etching the fiber end in hydrofluoric acid. The tips usually had a sub-micron end diameter with a smoothly tapered length of 500–1000 μm . Figure 1 is an SEM image of a typical tapered tip. The fiber tip was stepped into the biofilm in 20- μm steps, followed by an identical data set using a local effective diffusivity electrochemical microelectrode.⁹ Typical results are shown in Fig. 2. The data at 670 nm was normalized to the data at 1320 nm for the probe located outside of the biofilm, but still submerged in the solution. The microelectrode response is shown for comparison. The back-scattered optical signal at 1320 nm showed a large intensity variation (almost a factor of 5) as the tip moved through the biofilm towards the bottom. Moreover, the variations observed correlated well with the local effective diffusivity microelectrode. Further, the measurements at 670 nm showed a much smaller (<5%) intensity variation as the probe moved through the biofilm.

These results were highly repeatable. The correlation coefficient, R^2 , over many trials was always greater than 0.85. We also observed different, but repeatable calibration equations (with $R^2 > 0.85$) at different locations in the biofilm, presumably due to structural heterogeneity of the biofilm.

The dramatic wavelength dependence of the back scattered signal variations was unex-

pected. Mie scattering, the Mie effect¹⁰ and a strong water absorption band near 1.3 μm ¹¹ all play a role in explaining the observed behavior. The simplicity of the sensor and the large responsiveness in nominally transparent biofilms make it a promising candidate for routine laboratory use.

*Department of Electrical Engineering, Montana State Univ., USA

1. J.W. Costerton, Z. Lewandowski, D.E. Caldwell, D.R. Korber, and H.M. Lappin-Scott, *Ann. Rev. Microbiol.* **49**, 711–745 (1995).
2. A.B. Cunningham, B.M. Peyton, in *Applied bioremediation of petroleum hydrocarbons*, R.E. Hinchee, J.A. Kittel, H.J. Reisinger, eds., Battelle Press, Ohio, pp. 97–100 (1995).
3. P.D. Marsh, in *Microbial Biofilms*, H.M. Lappin-Scott, J.W. Costerton, eds., Cambridge University Press, New York, pp. 282–300 (1995).
4. C.I. Chen, M.A. Reinsel, R.F. Mueller, *Biotechnol. Bioeng.* **44**, 263–269 (1994).
5. W. Jec, Z. Lewandowski, P.H. Nielsen, W.A. Hamilton, *Biofouling* **8**, 165–194 (1995).
6. A.G. Gristina, *CMNEEJ* **16**, 171–178 (1994).
7. I. Klimant, G. Holst, M. Kuhl, *Limnol. Oceanogr.* **42**, 1638–1643 (1997).
8. S. Yang and Z. Lewandowski, *Biotechnol. Bioeng.* **48**, 737–744 (1995).
9. H. Beyenal, A. Tanyolaç, Z. Lewandowski, *Wat. Sci. Tech.* **38**, 171–178 (1998).
10. M. Born and E. Wolf, *Principles of Optics*, 6th ed. (Pergamon Press, Oxford, England, 1980).
11. M. Yarborough, in *Photonics Design and Applications Handbook* (Laurin, Pittsfield, MA 1996), pp. H287–H290.

CThL5

11:15 am

Super-resolution fluorescence microscopy by up-conversion-depletion using two color lasers

Y. Iketaki, T. Omatsu,* O. Sato,** T. Suzuki,** M. Fujii,[†] *Advanced Tech. Res. Ctr., Olympus Optical Co., Ltd. 2-3, Kuboyama-cho, Hachioji-shi 192-8512 Japan; E-mail: y.iketaki@ot.olympus.co.jp*

We propose a novel scanning fluorescence microscope capable of breaking the diffraction resolution limit by up-conversion process with two-color pump and erase lasers. Most of dye molecules with an S_1 state generated by irradiating of a laser (i.e., pump laser) decay to the ground state through fluorescence process.¹ On the other hand, the radiative relaxation of the molecules with a higher excited S_n state to the ground state is almost inhibited. By irradiating of pump beam and another laser (i.e., erase laser) for $S_n \leftarrow S_1$ photo-excitation at the same time, the molecules with the S_1 state are up-converted, and the fluorescence can be reduced. If the focused pump and erase beams are partially overlapped on a sample stained by dye molecules, the fluorescence from the region irradiated by both lasers is inhibited, as